Proceedings of ASME Turbo Expo 2011
GT2011
June 6-10, 2011, Vancouver, British Columbia, Canada

GT2011-46570

HEAT TRANSFER FOR THE FILM-COOLED VANE OF A 1-1/2 STAGE HIGH-PRESSURE TRANSONIC TURBINE—PART I: EXPERIMENTAL CONFIGURATION AND DATA REVIEW WITH INLET TEMPERATURE PROFILE EFFECTS

Harika S. Kahveci, Charles W. Haldeman, Randall M. Mathison, and Michael G. Dunn
The Ohio State University Gas Turbine Laboratory
Columbus, OH 43235

ABSTRACT

This paper investigates the vane airfoil and inner endwall heat transfer for a full-scale turbine stage operating at design corrected conditions under the influence of different vane inlet temperature profiles and vane cooling flow rates. The turbine stage is a modern 3-D design consisting of a cooled high-pressure vane, an un-cooled high-pressure rotor, and a low-pressure vane. Inlet temperature profiles (uniform, radial and hot streaks) are created by a passive heat exchanger and can be made circumferentially uniform to within ±5% of the bulk average inlet temperature when desired. The high-pressure vane has full cooling coverage on both the airfoil surface and the inner and outer endwalls. Two circuits supply coolant to the vane, and a third circuit supplies coolant to the rotor purge cavity. All of the cooling circuits are independently controlled. Measurements are performed using double-sided heat-flux gauges located at four spans of the vane airfoil surface and throughout the inner endwall region. Analysis of the heat transfer measured for the uncooled downstream blade row has been reported previously.

Part I of this paper describes the operating conditions and data reduction techniques utilized in this analysis, including a novel application of a traditional statistical method to assign confidence limits to measurements in the absence of repeat runs. The impact of Stanton Number definition is discussed while analyzing inlet temperature profile shape effects. Comparison of the present data (Build 2) to the data obtained for an un-cooled vane (Build 1) clearly illustrates the impact of the cooling flow and its relative effects on both the endwall and airfoils. Measurements obtained for the cooled hardware without cooling applied agree well with the solid airfoil for the airfoil pressure surface but not for the suction surface. Differences on the suction surface are due to flow being ingested on the pressure surface and re-injected on the suction surface when coolant is not supplied for Build 2. Part II of the paper continues this discussion by describing the influence of overall cooling level variation and the influence of the vane trailing edge cooling on the vane heat transfer measurements.

NOMENCLATURE

σ	Standard Deviation
A	Area
Avg	Average of Measurements (subscript)
C_p	Constant Pressure Specific Heat
f	With Film Cooling (subscript)
N_{phys}	Rotor Physical Speed
NSR	Net Stanton Reduction, $NSR = \frac{St_{\_0} - St_{\_f}}{\left|St_{\_0}\right|}$
$\frac{N_{phys}}{\sqrt{T_{0,\,inlet}}}$	Corrected Speed, N_{corr}
$\frac{P_{0,\,inlet}}{P_{0,\,outlet}}$	Total-to-Total Pressure Ratio
q"	Heat Flux
ref	Reference (subscript)
St	Stanton Number (global) $St = \frac{q''}{\frac{\dot{m}}{A_{ref}}[(C_pT)_{ref} - (C_pT)_w]}$
T	Local Temperature
u	Upper Gauge Measurement (subscript)
w	At a Wall Boundary (subscript)
	For St calculation in analysis, $T_w = T_u$
$\dot{m}$	Turbine Mass Flow Rate
0	Without Film Cooling (subscript)

1. INTRODUCTION

The primary goal of this effort is to experimentally determine the effects of inlet temperature profile and cooling levels on heat flux for the airfoil and inner endwall of the high-pressure vane of a turbine stage operating at design corrected conditions. It is a "macro" comparison of cooling in the presence of realistic complications such as inlet temperature profiles and interactions with a downstream rotor. As such, this study uses definitions of Stanton Number and effectiveness

based on global properties to trace the overall effect of cooling throughout the stage.

This paper is split into two parts, which are intimately connected. Care has been taken to avoid repetition between the parts. Part I sets up the experiment by focusing on the experimental configuration and providing a description of the control parameters of interest (cooling flow and vane inlet temperature profiles). It also presents a comparison of cooled heat flux measurements to data from an earlier experiment using the same geometry but without cooling. Part II of the paper focuses on the effects of cooling variation on the vane and endwall region and investigates the independent influence of the outer vane cooling circuit.

Both parts of the paper illustrate that while characterizing cooling flow as a function of parameters such as blowing ratio is a good way to think about the data from a fluid mechanics standpoint, it can be difficult to generalize these methods to a real engine environment. The number of cooling holes and the changes that occur as the cooling moves over and through the vane means that every cooling hole has its own blowing ratio, jet velocity, and temperature ratio. Further, interaction with the downstream rotor causes each of these parameters to change dramatically as a function time. While it may seem impossible to characterize the flow in this situation, looking at the "Macro" effects through a global definition of Stanton number and effectiveness shows where cooling is more or less effective, given changes in the overall stage boundary conditions.

This is a different approach from many other important studies that focus on the "micro" effects of cooling such as film layer establishment and the changes immediately downstream of cooling holes in an extremely controlled environment. Both of these approaches answer important questions, but they use very different processes to arrive at their conclusions and are often better suited for one type of experiment versus another. When they are combined, they add more understanding to what is happening in the engine than either method does by itself.

The data provide a good illustration of the impact of cooling on vane heat transfer for an operating turbine stage and can help guide code developers and other researchers by highlighting regions of the flow that are not well understood from a macroscopic properties perspective. Our understanding is weakest where effects of cooling are not well described by changes in the bulk temperature and cooling flow additions, and it is in these regions that further study is necessary.

2. LITERATURE REVIEW

In order to avoid repetition, the two parts of this paper address two different aspects of the immense topic of film cooling research. Part I summarizes previous work from a range of researchers to illustrate how our understanding of cooling has changed as facilities have become more capable of capturing the physics of operational engines. Part II builds on this and focuses more on the different perspectives used in film cooling research. The combined discussion is intended to provide context for the differences between those properties which are known well in an engine condition (the Macro properties) and those that need to be known well for more detailed fluid work (the Micro properties).

A significant portion of film cooling research has been performed using simple flow geometries, such as flat plates, or more realistically cascades dealing with stationary airfoils where rotational and unsteady effects may be generated to some extent. Rotating turbine configurations represent the engine environment as closely as can be done under controlled laboratory conditions by matching non-dimensional parameters at operating conditions. However, to this point in time, there is very little film cooling work done using full-scale turbine stages, because of many experimental difficulties that must be overcome.

There are several review papers providing valuable sources of information regarding film cooling. Goldstein [1] performed one of the earliest reviews that covered the discrete film cooling research until 1971. Beyond 1971 until 1998, Kercher provided a review for film cooling at the leading edge [2], and film cooling CFD efforts [3]. Elovic and Koffel [4] presented a review on the state-of-the-art (1983) design of turbine cooling systems. Simoneau and Simon [5] discuss the turbine gas path heat-transfer experiments and computational work for cascade and rotating rig configurations performed until 1993. Bunker [6] in 2000 presented a review for turbine blade tip heat transfer. A review of literature regarding turbine heat transfer and aerodynamics is reported in Dunn [7], which includes discussion of rotating turbine experimentation up to 2001.

Film-cooling experiments utilizing rotating configurations are few in number. Dring et al. were the first to report a film-cooling study that included rotation [8]. They compared measurements from a large-scale rotating blade with four cooling holes to previous flat plate and cascade data. Their findings suggested that suction surface film cooling behavior was similar to the non-rotational cases, but the pressure surface experienced a more rapid decay in effectiveness due to curvature and radial flow.

Later, Dunn performed measurements of heat flux distributions for a high-pressure turbine with slot injection at the vane trailing edge. He found that the presence of the rotor increased the heat transfer on the vane trailing edge by up to 25% but did not observe a significant effect for the rest of the vane mid-span [9]. A later study for the same turbine showed that the vane injection increased downstream blade leading edge heat flux both experimentally [10] and computationally [11]. However, in another experiment performed for the Teledyne CAE 702 HP turbine, Dunn and Chupp [12] observed that the vane injection had no influence on blade heat flux. They attributed this to the differences in the turbine aerodynamics and the injection techniques used for the two stages.

Takeishi et al. compared film-cooling effectiveness measurements for a high-speed rotating rig and a low-speed linear cascade using the same airfoil shape with leading edge, suction surface, and pressure surface cooling [13]. Their results agreed with Dring et al. that the film cooling effectiveness in the leading edge region of the pressure surface decayed more rapidly for the rotating experiment than the cascade measurements.

They concluded that this was due to the radial flow effects and high mixing occurring on the pressure surface.

Abhari and Epstein obtained unsteady heat-transfer measurements for the film-cooled blades of a transonic rotating turbine stage [14]. High blowing ratios were observed to decrease effectiveness, being in agreement with previous studies. Heat transfer was affected by the unsteadiness caused by blade row and wake-blade interactions, especially near the front of the blade. This resulted in an unsteady coolant performance. More recently, Haldeman et al. [15, 16] presented time-averaged and time-accurate measurements for a turbine with a cooled vane and blade row. The vane inlet temperature profiles and both the vane and the blade blowing ratios were varied, while the design corrected conditions were matched. Although the blade heat-transfer measurements were performed at several different span locations and in the tip/shroud region, the vane was only instrumented at mid-span.

Other more recent papers have combined migration studies and vane cooling studies. The work of Ong [17] and of Povey [18, 19] have all dealt with hot streak migration through a vane. The work of Pau [20] has described some of the issues surrounding platform cooling.

The current experiment has previously been described in two multi-part papers focused on the heat transfer for the uncooled downstream rotor [21, 22]. References are provided for the first part of each of these papers. Temperature profile effects were found to be more significant than cooling flow effects, and the vane outer cooling circuit (which supplied the vane trailing edge slots) was found to have the greatest influence on the blade heat transfer. Cooling had more impact on the suction surface of the blades than the pressure surface.

This data set is of interest to the gas turbine community since it is the first detailed vane heat flux data to include cooling and profile effects with a rotating turbine. The vane studied has a dense cooling scheme (nearly 300 holes per vane) both at the endwall and on the airfoil surface and is heavily instrumented with heat-flux gauges at several different spans and on the inner endwall. This range of data is even more critical as today's endwall designs are driven towards a contoured shape for performance benefits, and developing an understanding of the endwall contour on heat transfer first requires a detailed knowledge of endwall physics and film cooling interaction.

3. EXPERIMENT DESCRIPTION

The setup and orchestration of this experiment has been described in detail previously [22, 23] so only a brief overview will be provided here. However, it is important to note that the experimental apparatus is designed to capture all the complexities of a modern engine: the different vane inlet temperature profiles, the effect of cooling, rotation effects, and the manufacturing variation that occurs in the hardware. In looking for the macro effects of cooling, all of these issues play a role, even if they are not well documented in simpler and more controlled facilities. The turbine stage is incorporated into a specially designed housing illustrated in Figure 1 and the assembly is installed in the Turbine Test Facility.

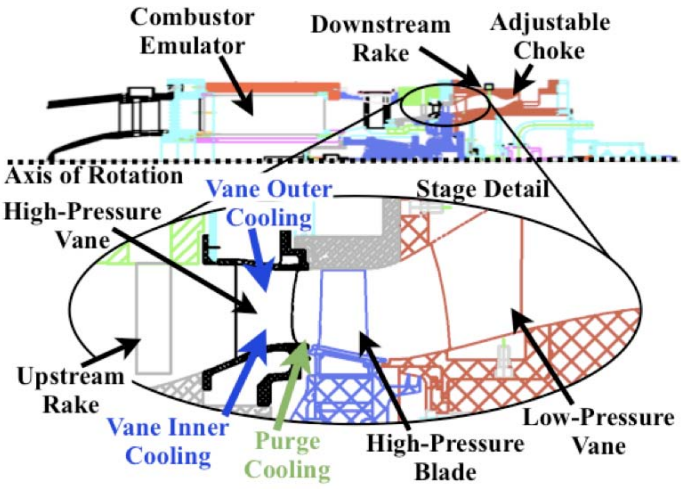

Figure 1. Turbine stage and housing schematic

High-pressure air enters the stage housing and passes through a passive heat exchanger referred to as the combustor emulator that is designed to create uniform, radial or hot streak temperature profiles by energizing different heater rods as is explained by Haldeman et al. [24]. Four different profiles are selected: uniform, radial, hot streaks aligned with the vane leading edge, and hot streaks aligned at vane mid-pitch. In keeping with realistic engine conditions, the hot streaks are created at half the number of vanes (one hot streak every two vanes). Bulk average temperatures are changed for different profiles to track the effect of profile shape versus bulk average temperature. This heated air then enters the turbine stage.

Coolant is supplied to the vane airfoil, the inner and outer endwalls, and the purge gap between the vane and the front face of the rotor disc from a separate low-temperature blowdown facility. The rotor blades are solid metal, as are the downstream low-pressure vanes. There are 38 high-pressure vanes, 72 high-pressure blades, and 38 low-pressure vanes.

Two sets of temperature and pressure rakes measure the conditions of flow entering and exiting the stage. The inner and outer vane coolant cavity temperatures and pressures are measured using miniature butt-welded thermocouples and Kulite pressure transducers for coolant mass flow calculations. Resistance temperature devices (RTDs) mounted inside the instrumented vane airfoils give an additional measure of the wall temperatures. Using the two internal thin-film heaters placed inside these vane airfoils, the wall temperature was varied during portions of the experimental matrix to obtain adiabatic wall temperature measurements. The outer endwall has cooling holes, but that portion of the vane row was not instrumented.

3.1 Vane Heat-Flux Instrumentation

Eight out of thirty-eight vane airfoils are instrumented with double-sided Kapton heat-flux gauges at four spanwise positions. The 5%, 15% and 90% span instrumentation are located on one single airfoil per each span, and 50% span and inner endwall measurements are distributed over multiple airfoils. Each Kapton gauge consists of a polyimide (Kapton) insulating substrate and two thin-film nickel resistance thermometers

bonded on opposite sides of this substrate, with a total thickness of 0.001 inches. The thermal conductivity of the Kapton was extensively measured most recently by Hodak [25] and is 0.23 W/m-K. The lower gauge measures the metal temperature, as it is in thermal contact with the surface, while the upper gauge captures the external flow field dynamics. Since the temperature on both sides of a substrate are known, the heat flux can be calculated. These gauges have a high frequency response on the order of hundreds of KHz, which makes detailed time-accurate measurements possible. The processing of the time-based temperature signals to heat flux requires a numerical algorithm that treats the thin Kapton substrate as a filter, affecting different frequencies inherent in the signal. This procedure has been well-documented by Cohen [26].

Temperature histories are shown for the upper and lower films of a typical heat-flux gauge in Figure 2. The main window shows the stable temperature that both the upper and lower sensors reach after the facility comes to its operating point. A typical data window covers two rotor revolutions, which requires approximately 15 ms. The insert shows the same measurements over the entire test-time. One can see the effects of the initial cooling being applied after about 400 ms as the temperatures drop slightly, and then the rise in temperature as the pressure builds in the hardware after the main flow is started. The same time window is indicated on the insert as well, which provides an indication of where the data window is taken relative to the entire test.

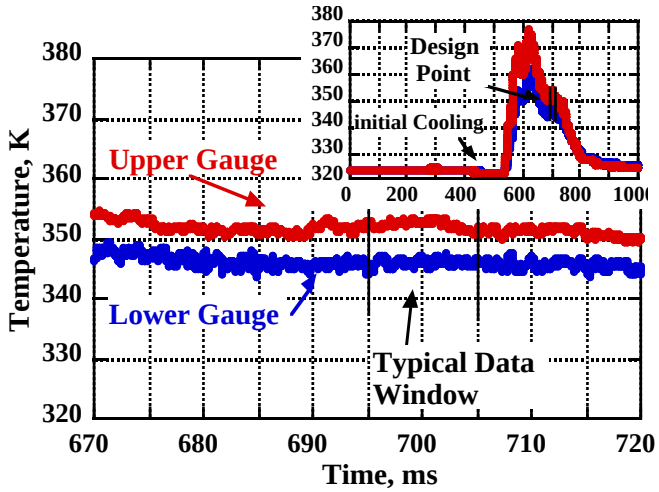

Figure 2 Typical Heat-flux Sensor Response

The full distribution of Kapton heat-flux gauge locations that provided measurements on the airfoil surface and on the inner endwall is shown in Figure 3. The blue circles on the airfoil layout and the crosses at the inner endwall show all available measurements (temperature and heat flux), regardless of gauges being in pairs or not. Heat-flux measurements were available for those gauges that had both upper and lower gauges active, shown with red circles on the airfoil surface, and red rectangles at the inner endwall.

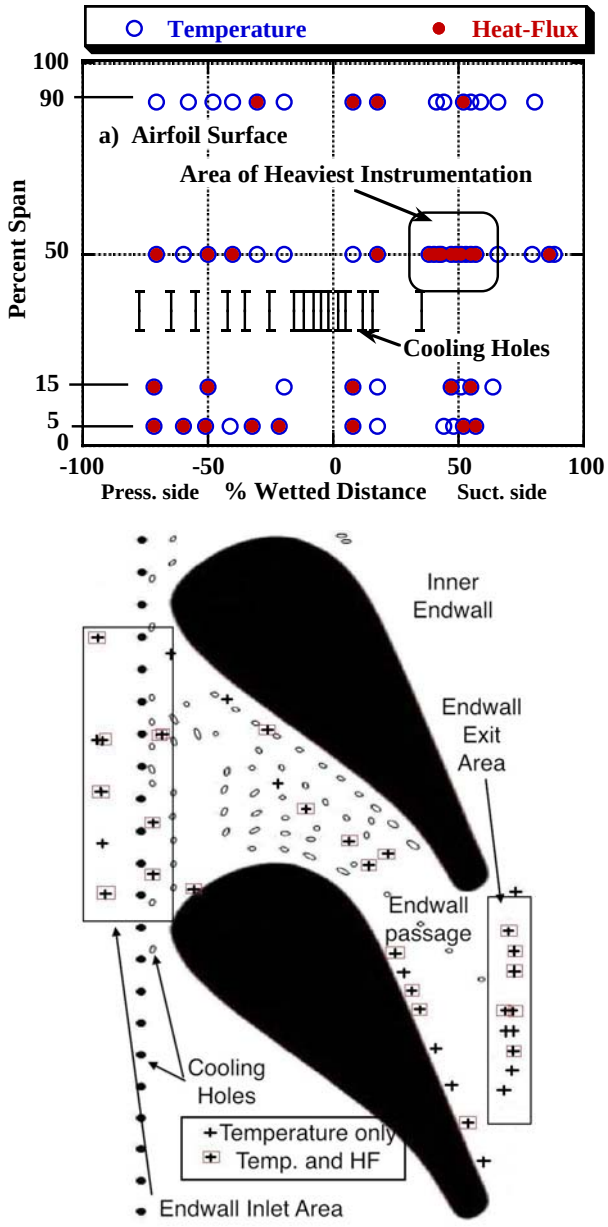

Figure 3. Vane heat-flux gauge locations on the (a) airfoil and (b) inner endwall (schematic not to scale)

In addition to the vane exit instrumentation, the area aft of the vane is instrumented heavily at the interface between the vane and rotating system where the purge flow joins the core flow. Pressure, heat-flux and temperatures measurements are available on both the stationary and rotating side. The effect of the purge flow is limited on the vane, but larger on the rotor hub area. More results for this area of the turbine stage can be seen in [21, 22].

3.2 Vane Film Cooling

Coolant is injected through perpendicular or angled circular cooling holes located on the vane inner and outer endwalls,

on the pressure and suction surfaces, and in a showerhead arrangement on the airfoil leading edge, as shown in Figure 4. There are seven rows of circular holes in the showerhead region, five of which are on the pressure surface. There are and additional six rows of holes further downstream on the pressure surface. On the suction side, in addition to the two rows of circular holes in the showerhead, there are two rows of fan-shaped holes slightly downstream and one more row of holes closer to the vane throat. There is also an array of cooling slots covering the full span of the pressure side of the trailing edge.

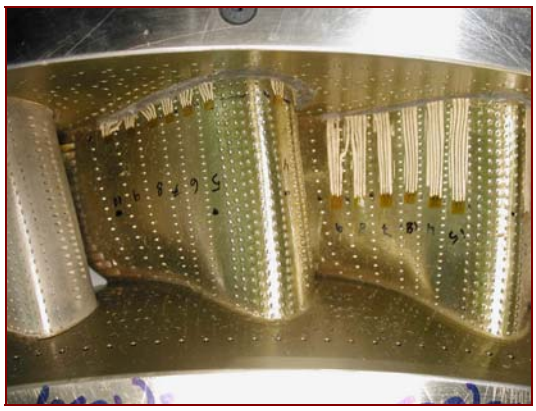

Figure 4. Cooling hole geometry on vane airfoil surface (not to scale)

Three independent cooling circuits supply the vane inner circuit, the vane outer circuit, and the purge cavity downstream of the vane. The vane inner circuit supplies the showerhead, the majority of the airfoil surface, and the inner endwall cooling. The trailing edge, last three rows of holes on the pressure surface, and outer endwall are supplied via the vane outer circuit. Details of the relative size allocation of cooling holes in each surface is discussed more in Part II of the paper, but most of the coolant from the vane inner circuit is used for the airfoil surface while a significant portion of the vane outer circuit coolant is supplied to the outer endwall.

3.3 Operating Conditions and Control Variables

The overall experimental matrix for this program has been described previously in [23], but the core component used for the work reported here consists of 36 experimental runs at similar corrected speeds and stage pressure ratios. Typical Reynolds numbers at the inlet to the vane are approximately 4.7E6 per meter. Table 1 summarizes this subset of runs by profile shape, the independently controlled cooling levels, and the status of the adiabatic wall temperature heaters as well as the runs that make up each condition. The profile types listed are uniform, radial, hot streak (HS), and cold. The cold runs are performed with an inactive combustor emulator, and the * on Runs 15 and 16 is to point out that the rotor was not spinning at the beginning of these runs. For the hot streak runs, additional information is provided about whether the hot streaks are aligned with mid-passage of the vane (MP) or with the vane leading edge (VLE) as well as whether the hot streak has a low, medium, or high magnitude. The cooling levels are described by *Off* (no coolant is supplied), *Nom* (nominal or design cooling flow rate), *Low* (lower than nominal flow rate), or *High* (higher than nominal flow rate). More information about these actual flow rates is provided in Part II of this paper. The last column indicates whether the wall heaters used to determine the adiabatic wall temperature are active or not. Only the rows labeled *On* have the heaters active.

It should be immediately clear that many runs are needed to fully cover the possible variable combinations in this matrix, and that even with the large number of runs used for this matrix, it is not feasible to have multiple repeat runs at each condition. For this reason, it was important to develop techniques to quantify data quality with only a single run, as discussed later.

Run	Temperature Profile	Vane Inner Cooling	Vane Outer Cooling	Purge Cooling	Adiabatic Wall Heaters
15,16*	Cold	Off	Off	Off	
20, 21		Off	Off	Off	
43, 47	Uniform	Off	Off	Off	
31		Nom	Nom	Nom	
32		Nom	Nom	Nom	
33		Nom	Nom	Nom	
49		Nom	Nom	Nom	On
22	Radial	Off	Off	Off	
17,23,24		Low	Low	High	
18,19		Low	Low	Off	
25		Low	Low	Nom	
40,41		Nom	Off	Nom	
26		Nom	Nom	Nom	
27,28		Nom	Nom	Nom	
44,45		Nom	Nom	Nom	On
50		Nom	Nom	Nom	
29,30		High	High	High	
46	HS-VLE (High)	Off	Off	Off	
42		Nom	Off	Nom	
35		Nom	Nom	Nom	
48		Nom	Nom	Nom	On
34	HS-VLE (Low)	Nom	Nom	Nom	
36	HS-VLE (Med)	Nom	Nom	Nom	
37	HS-MP(High)	Nom	Nom	Nom	
38	HS-MP (Med)	Nom	Nom	Nom	
39	HS-MP (Low)	Nom	Nom	Nom	

Table 1. Summary of operating conditions for vane heat transfer experiments

These runs can be grouped together by vane coolant flow rate to gain a better understanding of the impact of cooling on the turbine stage operation as done in Table 2. For each condition the range (maximum-minimum) is shown as well as the percentage of the actual value that the range represents. For the nominal cooling case the variation in total pressure ratio across 17 runs is about ±1.3%. The percent flow rate in each cooling

circuit with respect to the total flow is also given in Table 2, where the total flow is the exit mass flow (sum of core and coolant flows). The last row shows the decrease in the effective vane choke area as coolant is added to the system. The physical throat area did not change during the experiments, but the addition of coolant causes a blockage in the throat region, resulting in a decrease in the effective area. The overall variation in the total pressure ratio and corrected speed (largest to smallest) among the cooling levels is approximately the same as the variation within each cooling level. This implies that the effect of cooling on the overall performance is relatively small, although one can see that the majority of the difference occurs between the no cooling case and any cooling case.

Quantity	No Cooling	Low Cooling	Nominal Cooling	High Cooling
No. of Runs	4	6	17	2
Total-to-Total Pressure Ratio	4.62	4.53	4.59	4.56
	±0.12	±0.077	±0.06	±0.002
Range Range/Avg	±2.7%	±1.7%	±1.3%	±0.05%
N_{corr} (RPM/K^1/2)	373.9	364.5	371.9	369.4
	±11.2	±8	±8.2	±1.8
Range Range/Avg	±3.0%	±2.2%	±2.2%	±0.5%
V.I. Coolant % of Total	0	4.65%	6.89%	8.06%
Range (%)		±0.15	±0.40	±0.0
V.O. Coolant % of Total	0	4.35%	5.37%	6.28%
Range (%)		±0.14	±0.31	±0.0
Vane Area % of Uncooled	99.77]	94.92	90.88	90.43
Range (%)	±0.04	±0.02	±0.03	±0.01

Table 2. Summary of operating conditions by cooling level

Grouping the runs by profile shape for the nominal cooling level results in the temperature profile plots of Figure 5. These show the variation in the inlet conditions to the vane as a function of the profile heater set point. Each condition is an average of multiple runs, independent of cooling level. The data shown in part (a) is created by normalizing the measurements of each run by the average value (bulk temperature) for that run to produce a normalized temperature. These normalized temperatures are then averaged together by group (radial, uniform, hot streaks) and the range bars represent the variation within that group. Part (b) shows the same basic data, but now the data has been normalized by the same maximum average value among all groups. The maximum temperature occurs at the peak of the profile for the hot streaks aligned with the vane leading edge. The difference between these plots is that, in part (b), the relative magnitude of the temperature is preserved since it is a single scaling value. The larger range bars reflect that the bulk average temperature was intentionally varied among the runs. Part (a) removes this effect by normalizing each run by its average value. Here the range bars represent relative changes in shape, not the change in absolute level. This distinction is important as raw heat-flux measurements will change according to changes in the absolute temperature, but proper normalization through the Stanton Number should collapse the data down to provide just the effect of profile shape on the boundary layer.

Figure 5 shows the variation in profile shape for all runs grouped together by type. The variation in bulk average inlet temperature for the repeat runs shown in Table 1 are generally less than 1% of the average value. For example, for the radial nominal cooling case the variation between Runs 27 and 28 is only 0.02%, which corresponds to a ±0.1K variation in average inlet temperature, while a 0.27% variation for radial low cooling case (Runs 17, 23, and 24) means only ±1.43K. This suggests that the inlet temperatures in this series of experiments are very stable.

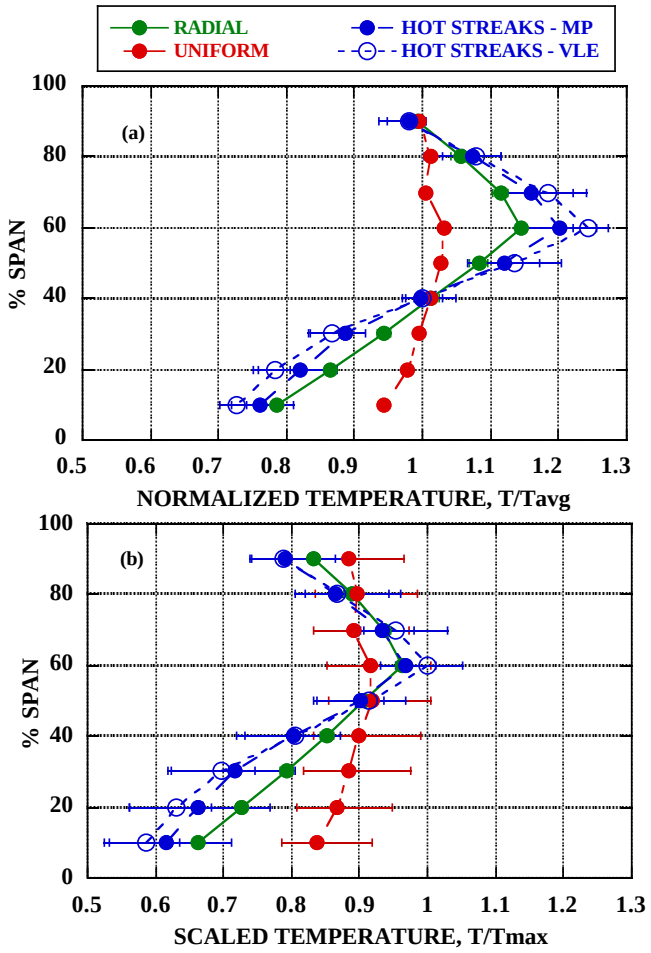

Figure 5. Inlet profiles for nominal cooling levels in terms of (a) normalized and (b) scaled temperatures

3.4 Stanton Number Definition and Use in a Fully-Cooled Environment

The heat flux measured by each gauge is a function of many variables that change dramatically through the vane such as the freestream fluid temperature, wall temperature, and velocity gradient. The key to any complex experiment where pro-

prietary geometry is involved is to find a method to present the data for the widest use, normalizing for changes in the main control conditions within the constraints of the geometry. It is expedient to find methods to account for local changes in values using readily available measurements such as the inlet temperature and mass flow rate, which are values commonly measured in actual engines.

One method to account for these effects and provide a more generally useful description of the measured heat flux is using a Stanton Number definition of the form provided in Equation 1.

$$St = \frac{q''}{\frac{\dot{m}}{A_{ref}}[(C_pT)_{ref} - (C_pT)_w]} \quad (1)$$

Previous papers have described a variety of methods of defining the variables in these equations along with the advantages and drawbacks of each case [15, 16, 27]. For the purposes of this paper, the principal definition of Stanton Number will use the measured heat flux for q", the sum of the core and vane inner cooling flows for the mass flow, and the effective vane choke area for the reference area. The current model does not account for the change in total mass flow across the vane as coolant is added from each row of holes. The denominator also includes the driving enthalpy difference between a reference temperature (T_{ref}) and a wall temperature (T_w). This definition accounts for profile shape by using the inlet temperature at the span corresponding to the gauge location as the reference temperature.

This definition of Stanton Number adopts a macro cooling perspective and highlights the global factors that drive the local heat flux. Locations for which the Stanton Numbers collapse well, given wide changes in the input conditions, imply that the main control variables are the driving temperature and the mass flow. Wherever the Stanton Numbers do not collapse well are the areas where the underlying boundary layers are being changed due to external conditions not related to mass flow or temperature.

For research needs more focused on micro cooling effects, it is common to define the Stanton Number based on local parameters to provide a picture of the change in heat flux due to velocity effects rather than changes in inlet temperature profile. This alternate definition has the same form as Equation 1, but uses the adiabatic wall temperature for the reference temperature. For this experiment, the adiabatic wall temperature is determined by fitting heat flux and wall temperature data from multiple runs with similar flow conditions but changing wall temperatures as described in detail in [22]. Because the adiabatic wall temperature is determined for each gauge, it represents the local fluid temperature just above the surface and helps remove the impact of cooling on fluid temperature. This definition helps in some venues and is a hindrance in others. It may be desirable to measure these local driving variables so that the heat transfer measurements for each gauge can be reduced to Nusselt Numbers or heat transfer coefficients, but the required measurements are difficult in any experimental environment and are exceedingly complex for the realistic geometry with hundreds of gauges and cooling holes described here.

Figure 6 provides a comparison of the principal Stanton Number definition used in this paper with a Stanton Number based on adiabatic wall temperature for the suction surface of the vane at 90% span.

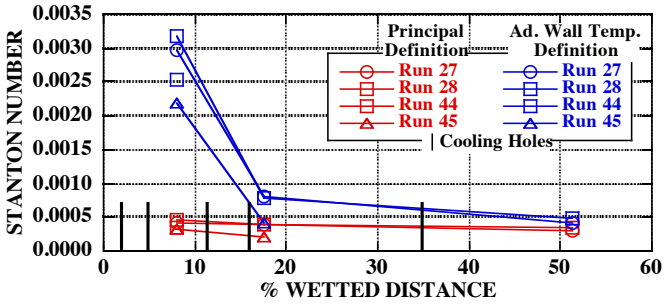

Figure 6. Comparison of Stanton Number definitions for suction surface at 90% span

This plot illustrates the difference in meaning between the two Stanton Number definitions. It includes data from the four runs used to generate the adiabatic wall temperature; Runs 27 and 28 have a very similar wall temperature, while Runs 44 and 45 have elevated wall temperatures to allow the determination of the adiabatic temperature. The principal definition for Stanton Number does a good job collapsing these changes between runs to a single point and creating a usable indicator of the heat flux that can be scaled for other environments. It will be shown later in this paper and in Part II that this definition is also effective at removing the small variations from run to run but highlighting changes in cooling level.

In contrast, the adiabatic wall temperature definition for Stanton Number shows a much more dramatic change over the surface of the airfoil because it accounts for the reduction in fluid temperature due to the introduction of cooling. While the principal Stanton Number definition shows that the heat transfer level stays reasonably constant over the vane surface, the adiabatic wall temperature Stanton Number definition indicates that the point at 8% wetted distance would experience much more heat transfer if not for the fluid temperature reduction caused by the introduction of cooling flow. This gauge is strongly influenced by the large amount of cooling introduced in the leading edge region. The two cooling holes upstream of the 17.5% gauge also cause a difference between the two cooling definitions at that location. It is interesting to note that for the gauge at 51% wetted distance, the difference between the two definitions becomes small since the temperature reduction due to cooling has been largely mixed out. This type of comparison provides an indication of the adiabatic film cooling effectiveness. Film effectiveness could be calculated directly but would require better knowledge of the coolant temperature exiting the hole than is currently available for a vane with hundreds of holes.

The adiabatic wall temperature definition for Stanton Number does not collapse the repeat runs as well as the princi-

pal definition. This indicates that there are global factors at work in determining the heat flux that are not fully captured by this local definition. It can therefore be concluded that the local definition is not the perfect method to investigate this data either.

These comparisons show that there is real value in both Stanton Number definitions; each definition brings out different aspects of the data and neither definition provides a perfect technique. In choosing between these parameter definitions, there is not a wrong answer, but each option points to a different kind of study. The principal Stanton Number definition using the inlet temperature will be used throughout the rest of this paper because the current study is less focused on the near-hole interactions observed by gauges immediately downstream of cooling rows and more interested in the macro-scale migration and coverage of cooling flows. This definition provides a normalized indicator of the measured heat flux that shows cooling effects and can easily be scaled to other questions of interest. In addition, the methodology for calculating this Stanton Number only requires data from a single run, is more readily applied to a wider variety of conditions, and can be used for data from older experiments where the adiabatic wall temperature is not available.

3.5 Stanton Number Reduction

For future comparisons, only the global definition of Stanton Number will be used as a representative of the scaled heat flux. Comparisons among different cases will highlight the impact of changes in cooling level and other factors. One useful method for making these comparisons is using the Net Stanton Number Reduction relationship defined in Equation 2.

$$NSR = \frac{St_{\_0} - St_{\_f}}{|St_{\_0}|} \quad (2)$$

In this case, the NSR compares one situation (with film cooling) to another (without film cooling) to highlight the relative change, even when the effects are small, such as in comparing the effects of cooling at slightly different mass flow amounts. As shown in Equation 2, the traditional definition is modified to account for cases where one of the two cases might have negative numbers (typically seen at the hub in the radial cases) by using the absolute value of the Stanton Number. This technique will be used in Part II of this paper when comparing the difference between cooling cases.

4. DATA QUALITY AND REPEATABILITY

4.1 Measurement Repeatability

In general, the instrument precision errors (due to calibration and processing techniques) were found to be much lower than the measurement repeatability for all sensors, which in turn was smaller than the variation between inlet conditions [27]. Thus, repeatability of the inlet conditions is used throughout the data analysis as an indicator of the overall accuracy of the experimental conditions.

The Kulite pressure transducers have a calibration accuracy of ±0.2 psia (±1.5 kPa), and the RTD's are calibrated in an oil bath to an accuracy of ±0.1 K. Typical calibration accuracies through the A/D system are about ±0.3 K. The run-to-run variation in the mass flow was found to be less than ±2% of the exit mass flow for the majority of the runs.

The variations in the temperature measurements from the heat-flux gauges at the target point differ from run-to-run. For radial nominal cooling repeat case (Runs 27, 28), the average variation for all the upper and lower gauges at all spans is only 0.32% of the average measurement among repeat runs. Although the variations in temperature measurements are very small among repeat runs, the heat-flux calculations give significantly larger variations. The heat flux errors determined by a traditional error propagation technique are estimated to be on the order of ± 1.5%, and This implies that the run condition stability and the resolution of the heat-flux sensors at these low levels of heat transfer are the ultimate limiters of heat flux accuracy (more detail are available in [27]). Generally, there is a ±4000 W/m^2 variation among repeat runs on the airfoil surface (about 8% variation). Examining just the Stanton Number and variation from repeat runs, the average value of all the values on the airfoil is about 3x10^{-4}. The repeatability is normally distributed and the values are well within the ±3x10^{-5} limits (or within 10%) of the average value.

4.2 Stanton Number Uncertainty

The definition of Stanton Number incorporates a driving temperature (the difference between the upstream rake temperature and the local fluid temperature) in the denominator, which is actually the main driver in the Stanton Number uncertainty. Figure 7 shows this distribution for arbitrarily selected runs with different cooling levels and temperature profiles. This shows that the overall uncertainty in the Stanton Number is not just an artifact of the uncertainty in the heat-flux measurement, but also the test condition.

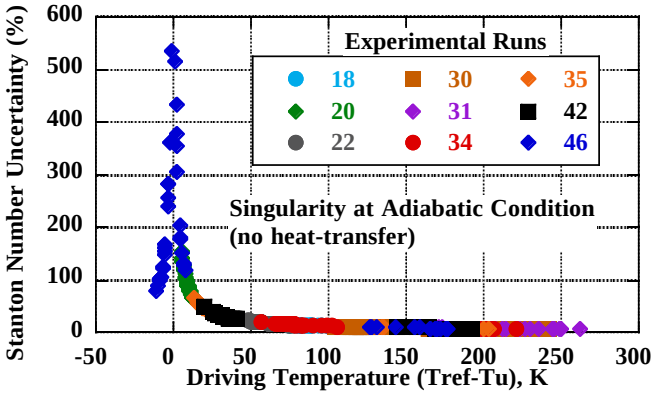

Figure 7. Uncertainty in Stanton Number calculation

This finding suggests that to ensure reliable Stanton Number normalization, the temperature difference introduced by the inlet temperature profile should be adjusted in such a way that the temperatures at the inlet stays higher than the corresponding local fluid temperatures on the airfoil surface. Highest uncertainty levels are generally observed for the cold runs and hot streak runs at the inner endwall and at 5% span. These runs

have essentially no driving temperature or heat flux. They are close to the adiabatic condition and therefore have Stanton Numbers very close to zero.

4.3 Multivariable Regression (Statistical) Modeling

An innovative technique was used to quantify the variation in the inlet temperature profiles for these experiments. Using traditional statistical modeling practices, multiple runs with independent operating conditions can be used to quantify the variation, without requiring multiple repeat runs. One of the key findings of this work is that taking the range of the experimental measures for repeat conditions often comes quite close to a more stringent statistical analysis generally used to establish the 95% confidence limits, providing a quick check on data quality without resorting to detailed statistical work.

The essence of the problem is that traditional cooling experiments have a large number of control variables. In this experiment the number of independent control variables is on the order of a dozen, and approximately 36 experiments focused on the vane were performed. A few conditions do have repeat runs, as shown in Table 1. However, to do a full statistical description of each condition would require many more runs at each point. The number of runs depends on the use of statistical descriptions, but using the Student's T statistic, one can achieve corrected 95% confidence limits for any number of runs based on the calculated standard deviation of the data, although typically five to ten runs per point would not be excessive.

If one uses only five runs per condition and has a dozen control variables (not all of which will be changed independently but many will), a typical experimental matrix could easily run into the hundreds of runs. This becomes difficult to achieve since the instrumentation does not generally have that type of life expectancy. A solution to this problem comes from the social sciences, which routinely use multivariable regression (statistical models) to describe empirical relationships between variables. The social sciences generally use this approach to determine if one variable is related to another, but for our case we can use the variation of the model from the data to form the basis for 95% confidence limits. The benefit of this technique is that one can use all of the runs to help quantify the variation for any run, but the cost is that in addition to the variability in the ideal repeat conditions, the results also include the variation from the model. This means that quantifying the variation using statistical modeling across multiple different conditions provides a more robust measure of the confidence limits, it can help isolate instrument problems that may occur throughout the test matrix, and it can highlight areas of the flow where the functional descriptions are less understood. The use of this technique will be highlighted by looking at the variation in the inlet temperature profile shapes. This technique has also been used to describe the variation in the heat-flux measurements, but that analysis is too detailed to present here.

The inlet temperature profiles are a good case for demonstrating the benefits of this technique, since they are not impacted by most of the control variables. Thus, there are many repeat runs, which can also be analyzed using the traditional statistical description for comparison. One can see from Table 1 that there are 8 repeat runs for the nominal cooling with radial vane inlet temperature profile case (17 if the profiles are considered independent of cooling).

Figure 8 shows all the radial temperature profile shapes at different cooling conditions, each shown with a different color. The data points show the average of the repeat runs (only a couple) over the two rakes. The range bars show the maximum-to-minimum range from the average for the experimental data, and 95% confidence limit for the statistical data generated using the "R" statistical processing software.

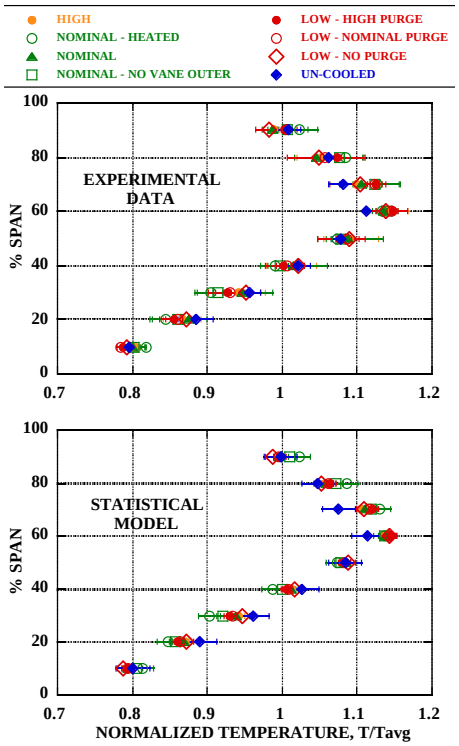

Figure 8. Temperature profiles as (a) measured experimentally and (b) statistically modeled

The data is given in the form of normalized values using the bulk average temperature of each run. The statistical model results look very similar to the experimental data. The experimental results use only the repeat runs in each profile shape, but the statistical model uses all available runs for calculations, resulting in dramatically improved confidence limits distributed over different span locations. This is the primary benefit of statistical analysis, as the confidence limits for even a single run can be predicted using all available runs. These confidence limits are useful both for describing the experimental data and for allowing computational modelers to include boundary condition uncertainty in determination of the propagated uncertainty in predictions.

Figure 9 shows a comparison of the variations in the data calculated on the basis of only the repeat runs by looking at the statistical description of the data: the calculated 95% confi-

dence limits (blue, ±4σ, using a T statistic correction for the smaller number of runs), the range bars (red) for the experimental data, and the 95% confidence limits based on the statistical model covering all runs (green). In this figure, just one case is shown for the nominal cooling at 50% span, but the results are consistently independent of span location or cooling level. In all cases, the experimental uncertainty is better represented by the range than some function of the standard deviation which overestimates the uncertainty dramatically.

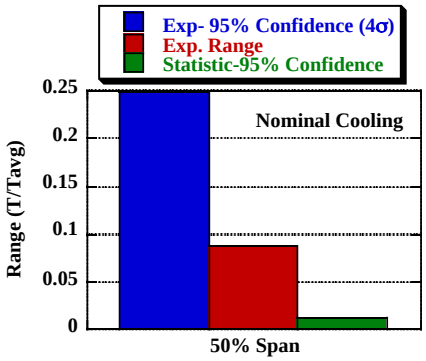

Figure 9 Comparison of statistics with experimental data

The practical importance of this finding is significant. For complicated experimental conditions, one now has two methods for estimating the 95% confidence limit. For limited repeat runs, the range of the variation approaches the typical 95% confidence limit. This avoids large overestimates that come from taking standard deviations over small numbers of samples. Alternatively, simple statistical modeling using software packages such as "R" can be used to group different run conditions together to come up with more traditional 95% confidence limits. Both of these provide reasonable estimates without having to expand the experimental matrix with many repeat run conditions.

5. OVERALL COOLING EFFECT

The overall cooling effect can be seen on the vane airfoil surface and at the inner endwall by comparing three different conditions: the Build 2 cooled case (Runs 31, 32, 33), the Build 2 un-cooled case (Runs 43, 47), and the Build 1 un-cooled case (using the same turbine hardware with no cooling scheme). Since the combustor emulator was created for the Build 2 experiments to generate non-uniform profiles, only a uniform profile is available for the earlier Build 1 data and all subsequent comparisons must focus on this profile type. Figure 10 provides a comparison of the inlet temperature profiles for the uniform runs. The data points in blue show the averages of six runs from two inlet rakes for Build 1 for which the operating design conditions (pressure ratios, inlet temperatures, and the corrected speeds) were matched with those of Build 2 uncooled runs, and the data points in red show the averages of two runs from two inlet rakes for Build 2. The average temperature used for the normalization is the average of both rakes at all spans. The variations among all these measurements are presented with range bars. The smaller variations obtained at the inlet profile with Build 2 shows how the overall quality of the repeatability has generally improved over Build 1 data. Clearly, the inlet temperatures match well for the two cases and the small differences that exist are well within the instrument ranges of the Build 1 data.

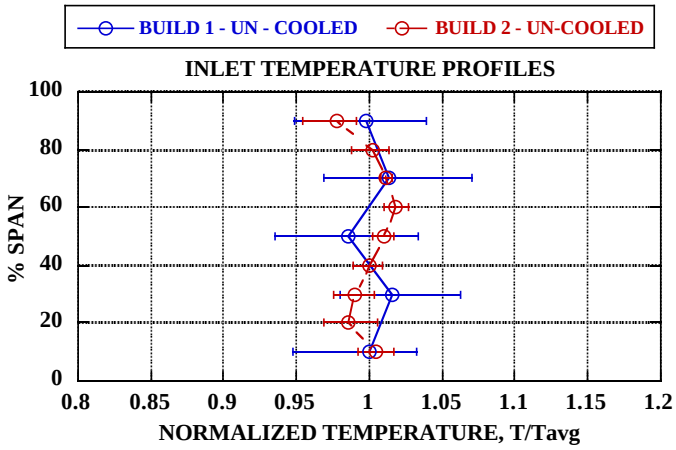

Figure 10. Comparison of inlet temperature profiles for Builds 1 and 2

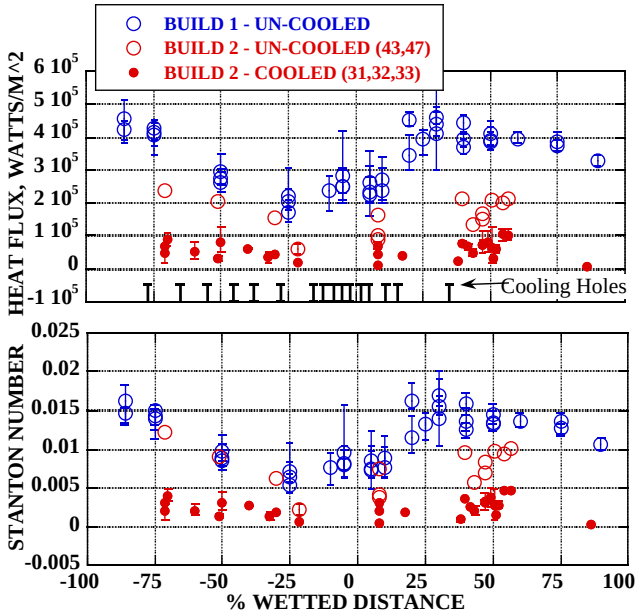

Figure 11. Impact of cooling on vane airfoil

Figure 11 shows the heat transfer on the airfoil surface in terms of raw heat flux and Stanton Number distributions for the three cases of interest. The Stanton Numbers shown for this comparison are calculated using the definition originally used for the Build 1 data and are much higher than the levels presented in the rest of this paper. For this definition only, the reference area and the reference temperature are taken to be the vane inlet area and the average temperature from both rakes, respectively. Measurements at all spans are combined together to reveal the trends more clearly via generating a denser distri-

bution of data points. The variation by span location, while influencing the heat flux, does not influence the Stanton Number greatly [27]. The raw heat flux shows three distinct levels with the Build 2 cooled values running below the Build 2 uncooled values, which in turn is lower than the Build 1 data. However, once the data is converted to Stanton Number, the Build 2 and Build 1 un-cooled data align on the pressure surface. After about 35% on the suction surface, the un-cooled Build 2 data starts to track lower than the original Build 1 data (about halfway between the cooled Build 2 and the Build 1 data). This result is an indication of air being ingested through the pressure surface cooling holes and being ejected out of the suction surface cooling holes for the un-cooled case. For the Build 2 un-cooled runs, the coolant was simply not supplied, but the cooled hardware was in place. There is no evidence that the amount being ingested affects the pressure surface heat transfer, and the resulting low mass flows through the airfoil ensure that the gas being ejected is almost certainly close to the metal temperature.

The comparison between these three cases provides interesting engineering data:

1) It is important to note that the instrumentation on the Build 1 vane is completely different than used for Build 2. For Build 1, the measurements were performed using traditional Pyrex single sided heat-flux gauges. Build 2 data were obtained using the Kapton double-sided heat-flux gauges and utilized different calibration and data reduction techniques. The fact that they align so well on the pressure surface, on two different pieces of hardware, obtained years apart, provides a high degree of validation for the Kapton sensors.
2) On the suction surface, the Build 2 un-cooled data has three values at 10% wetted distance. One lines up well with Build 1 data. This is in an area with lots of cooling holes, but the fact that it does not track lower like its companions further downstream points to the fact that there is little ejection going on in this location (low pressure variation), or that the definition of the Stanton Number used is still valid in this location. However the other two are very close to the cooled values. This indicates that this area seems to be very sensitive to changes and the values seem to change between the cooled and uncooled levels.
3) The importance of using the Stanton Number in these types of experiments cannot be overestimated. The picture one would get by just looking at the heat flux in Figure 11 is different than that shown by the Stanton Number. Looking at the raw heat flux would suggest that the Build 2 un-cooled data was substantially lower than the Build 1 data everywhere, which it is not once one accounts for the mass flow and temperature variations. The flip side is also very important; if the Stanton Number does not collapse the data in localized places, there is something about the flow that is not being accounted for, as seen at the aft end of the suction surface.
4) From a very practical perspective, the effect of cooling is dramatic, dropping the heat flux at most spans much closer to 0. As pointed out previously, this observation suggests that significant portions of the direct measurements for the cooled cases are obtained at conditions close to the adiabatic wall temperature.

A similar pattern is also shown in Figure 12 where the data along the endwall is compared both in terms of heat flux and in terms of Stanton Number. For this case only a small set of measurements are provided that can be compared directly to Build 1 data, which was less heavily instrumented in the endwall region. Once again, the raw heat flux data is lower for the Build 2 un-cooled data, but once converted to Stanton Number the data tends to line up within the range of the Build 1 data. There is very little sign of ingestion at the leading edge/ejection towards the trailing edge. The only exception may be the data just downstream of the vane trailing edge where the Stanton Number is running slightly lower for the Build 2 data; however, the effect is small. In comparison, the cooled data is essentially at the adiabatic wall temperature (zero heat-flux).

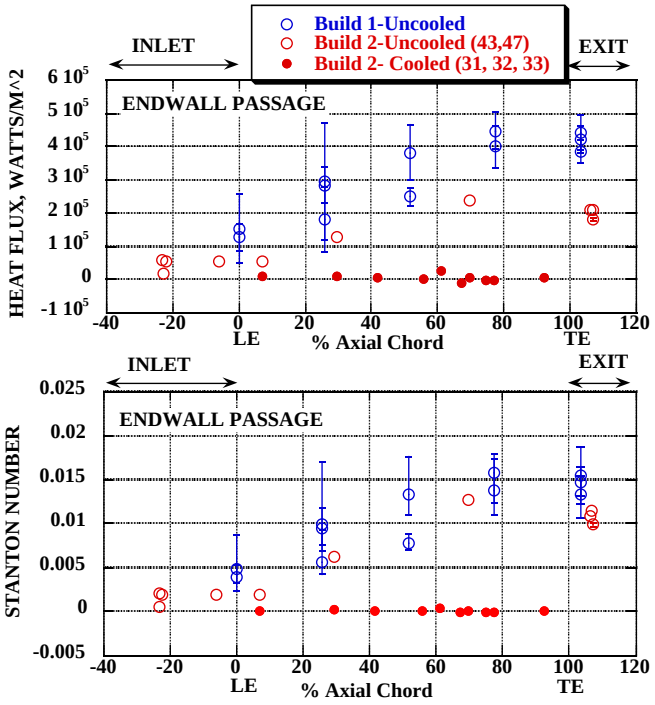

Figure 12. Comparison of un-cooled data at endwall

6. INFLUENCE OF INLET TEMPERATURE PROFILE

The impact of vane inlet temperature profile shape can be clearly observed on the vane airfoil heat-flux measurements and on the Stanton Number at the 50%, 15%, and 5% span locations (where sufficient data exists) as shown in Figure 13.

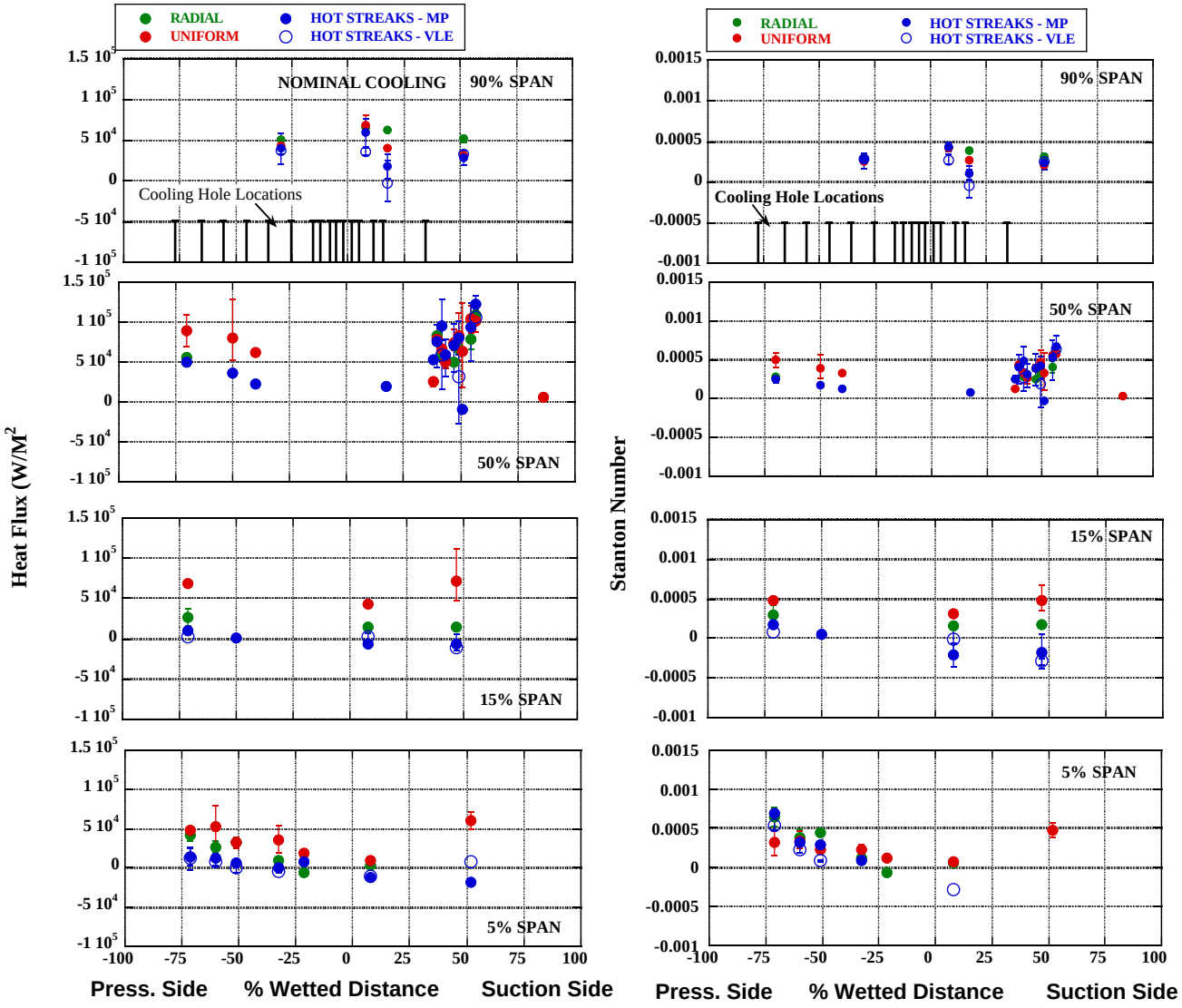

Figure 13. Stanton Number based on local temperature (various profile shapes) for nominal cooling

As one would expect, the radial and hot streak temperature profiles result in higher heat fluxes at midspan near the peak of the profile and lower values at the inner and outer spans where the inlet temperature is lower. Looking back at Figure 5b, one sees that the inlet profiles have a peak at about 60% span. At 50% span the profiles are about equal and everywhere else the uniform profile is hotter. The heat-flux values also decay with span position regardless of the profile shape with the higher values being at 50% and 90% span and the lower values towards the inner endwall.

The Stanton Number plots tell a more complete story than the raw heat-flux plots that can mask what is truly occurring. One sees that the wider range at any given span in heat flux tends to be reduced when examining the Stanton Number. The Stanton Number plots also show a noticeable reduction in the size of the range bars from the heat flux plots. Each condition is the average of several runs, and the range bars represent the variation over those runs. For instance, on the pressure surface at 50% span, the variation in the uniform condition is relatively large, but that range is diminished greatly when plotted as a Stanton Number. This shows that, as is the case for un-cooled heat transfer, Stanton Number does a good job of reducing run-to-run variation within a group even in the presence of cooling. One has to remember that the hot streak runs are perhaps the most difficult condition to know exactly what the reference temperature is, as the profiles are highly non-uniform in the circumferential direction, and the largest effect for this will be at the 50% span. The alternative viewpoint is that even with these unknowns and the fact that the profiles move a significant distance form the rakes to the vanes, the general use of the rakes as the reference temperature collapses the data, even in the presence of hot streaks.

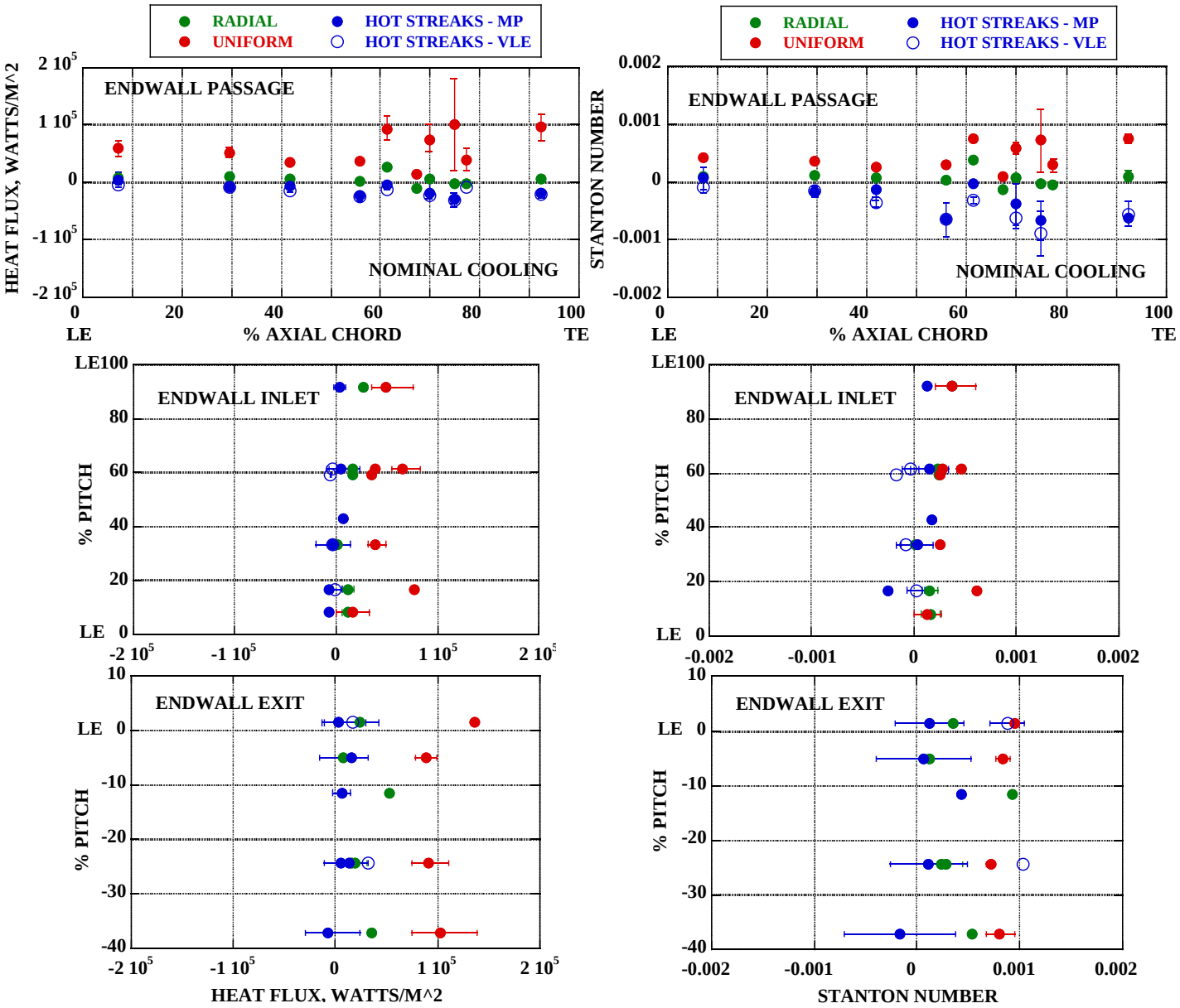

Figure 14 Inner endwall (a) heat flux and (b) Stanton Number

It is a different story when examining the endwall data. Figure 14a shows the endwall data first throughout the passage as a function of axial chord, and then the endwall inlet and the endwall exit data as a function of pitch position, respectively. For all these plots, the location of the vane leading edge is marked. Similar plots are shown for the Stanton Number data in Figure 14b. At the endwall, the heat-flux values are low, even for the uniform condition, but the conversion to Stanton Number tends to bring the uniform and radial runs together while accentuating the differences between the radial and hot streak runs. The endwall inlet, which is the region immediately upstream of the vane (as labeled in Figure 3), also shows a similar collapsing of the data. At the endwall exit, the amount of change between heat flux and Stanton Number is relatively small, and in fact the variation within each group of runs, seems to grow larger for the Stanton Number. The reason for this can be seen by examining the plots more carefully. Moving downstream through the passage, the Stanton Number definition does not account for the addition of coolant mass flow. As a result, the data diverges both within the passage and at the exit. While the reference conditions are notoriously hard to measure at the inner endwall and are most subject to error (the measurements are being propagated downstream from the rakes in the boundary layer), one can see that they still do a fairly good job collapsing the data for the vane inlet region, even with the addition of a little cooling. However, with increasing cooling and a larger percentage of the cooling flow being introduced through the passage, the normalization does not work as

well. This is a case where the failure to collapse the data is indicative that the main changes in heat flux are not being driven by the bulk temperature or the mass flow, but the local conditions, which is most noticeably a localized cooling effect. If the Stanton Number as defined accounts for all of the key parameters, the different profile shapes should collapse on top of each other. While the differences among profiles are significantly reduced from what is observed for heat flux, there are still regions where the Stanton Number fails to fully account for the profile effect. These differences could be blamed upon shifts in profile shape between the inlet rakes and the vane, but companion computational studies do not predict substantial changes in profile shape upstream of the vane as was shown by Mathison et al. [28]. This suggests that one or more of the parameters used in defining the global Stanton Number do not accurately capture the local physics of the heat transfer as is traditionally done by using a more local definition of Stanton number.

While further investigations of the proper definition of Stanton Number may seem esoteric at first glance, the answer to this problem has value to a turbine designer. Achieving proper normalization of the heat-flux measurements is key to understanding which parameters drive heat flux at a specific location. One of the interesting results of this work is the approximate collapsing of the data that occurs based on the global properties. Being able to separate the macro from the micro effects allows the designers different controls to minimize cooling requirements with the minimum impact on other design considerations. Current understandings tend to lump multiple factors together, which provides a workable model but also makes it difficult to predict which design modification will make the biggest difference in a problem region.

7. SUMMARY

The experiment described herein required many new features such as the combustor emulator for heating the inlet flow, the incorporation of a coolant supply system, and the use of double-sided Kapton heat-flux gauges on the film-cooled vane. Despite these complex changes in experimental technique, comparisons of the un-cooled data from an earlier experiment using the same geometry profile (Build 1) with un-cooled data from the current experiment (Build 2) showed very good agreement on the pressure surface of the vane.

A significant difference between the two experiments is observed for the suction surface, since the vane cooling holes in Build 2 ingest flow on the pressure surface of the vane and inject it on the suction surface with a significant blowing ratio. This confirms that simply not supplying coolant to a component with cooling holes is not an accurate reflection of uncooled geometry. In addition, a comparison between the uncooled Build 1 data and the cooled Build 2 data showed a significant reduction in Stanton Number at all locations due to the introduction of cooling. Further analysis of different cooling effects is given in Part II of this paper.

In order to gain a better understanding of the uncertainty and repeatability of these measurements, a statistical technique commonly used in other fields is applied in a novel way to develop 95% confidence intervals for data from every run, even if repeat runs at the same condition are not available. This technique is critical for the new wave of complicated cooled-turbine experiments where it is not practical to perform multiple repeat runs at the myriad of conditions that must be investigated.

The impact of inlet temperature profile shape is observed in the heat-flux measurements for multiple spans of the vane airfoil. Attempts to normalize for this profile effect by calculating Stanton Number based on the inlet temperature at the appropriate upstream location did a reasonable job of collapsing data from different profile shapes. Further work in this area will be necessary to develop a more representative Stanton Number and gain a better understanding of the factors driving local heat transfer, especially on the inner endwall.

8. ACKNOWLEDGEMENTS

The authors are very appreciative of the hard work of the technical staff of the Gas Turbine Laboratory and the support of the GE Aviation University Strategic Alliance Program. The authors would like to especially thank the GEA technical monitor, Dr. Robert Bergholz, for his technical support, guidance, and patience throughout this research, as well as Dr. Christopher Holloman of OSU for performing the statistical analysis of the data.

9. REFERENCES

1. Goldstein, R.J., ***Film Cooling***, in Advances in Heat Transfer, T.F. Irvine and J.P. Hartnett, Editors. 1971, Academic Press: New York. p. 321-379
2. Kercher, D.M., 1998, "***A Film-Cooling CFD Bibliography: 1971-1996***", International Journal of Rotating Machinery, **4**(1): pp. 66-72.
3. Kercher, D.M., 2000, "***Turbine Airfoil Leading Edge Film Cooling Bibliography***", International Journal of Rotating Machinery, **6**(5): pp. 313-319.
4. Elovic, E. and Koffel, W.K., 1983, "***Some Considerations in the Thermal Design of Turbine Airfoil Cooling Systems***", International Journal of Turbo and Jet-Engines, **1**: pp. 45-66.
5. Simoneau, R.J. and Simon, F.F., 1993, "***Progress Towards Understanding and Predicting Heat Transfer in the Turbine Gas Path***", International Journal of Heat and Fluid Flow, **14**(No 2): pp. 106-128.
6. Bunker, R. "***A Review of Turbine Blade Tip Heat Transfer"***. in International Symposium on Heat Transfer in Gas Turbine Systems. 2000. Izmir, Turkey
7. Dunn, M., 2001, "***Convective Heat Transfer and Aerodynamics in Axial Flow Turbines***", ASME Journal of Turbomachinery, **123**(October): pp. 637-686, (Original Publication: 2001-GT-0506).
8. Dring, R.P., Blair, M.F., and Joslyn, H.D., 1980, "***An Experimental Investigation of Film Cooling on a Turbine Rotor Blade***", Journal of Engineering for Power, **102**: pp. 81-87.

9. Dunn, M., 1985, "***Turbine Heat-Flux Measurements: Influence of Slot Injection on Vane Trailing Edge Heat Transfer and Influence of Rotor on Vane Heat Transfer***", ASME Journal of Engineering for Power, **107**: pp. 76-83, (Original Publication: 84-GT-175).
10. Dunn, M., 1985, "***Heat-Flux Measurements and Analysis for a Rotating Turbine Stage***". Paper 16, AGARD-CPP-390.
11. Metzger, D., Dunn, M., and Hah, C., 1991, "***Turbine Tip and Shroud Heat Transfer***", ASME Journal of Turbomachinery, **113**: pp. 502-507, (Original Publication: 90-GT-333).
12. Dunn, M.G. and Chupp, R.E., 1989, "***Influence of Vane/Blade Spacing and Cold-Gas Injection on Vane and Blade Heat-Flux Distributions for the Teledyne 702 HP Turbine Stage***", AIAA J Propulsion and Power, **5**(2): pp. 212-220.
13. Takeishi, K., Aoki, S., Sato, T., and Tsukagoshi, K., 1992, "***Film Cooling on a Gas Turbine Rotor Blade***", ASME Journal of Turbomachinery, **114**(4): pp. 828-834, (Original Publication: ASME 91-GT-279).
14. Abhari, R.S. and Epstein, A.H., 1992, "***An Experimental Study of Film Cooling in a Rotating Transonic Turbine***". 92-GT-201, IGTI-Turbo Expo, Cologne, Germany.
15. Haldeman, C.W., Dunn, M.G., and Mathison, R.M., 2010, "***Fully-Cooled Single Stage HP Transonic Turbine: Part II - Influence of Cooling Mass Flow Changes and Inlet Temperature Profiles on Blade and Shroud Heat-transfer***". GT2010-23445, ASME Turbo Expo 2010, Glasgow, Scotland.
16. Haldeman, C.W., Dunn, M.G., and Mathison, R.M., 2010, "***Fully-Cooled Single Stage HP Transonic Turbine: Part I - Influence of Cooling Mass Flow Variations and Inlet Temperature Profiles on Blade Internal and External Aerodynamics***". GT2010-23446, ASME Turbo Expo 2010, Glasgow, Scotland.
17. Ong, J. and Miller, R.J., 2008, "***Hot Streak and Vane Coolant Migration in a Downstream Rotor***". GT2008-50971, ASME Turbo Expo 2008, Berlin, Germany.
18. Povey, T., Chana, K.S., Jones, T.V., and Hurrion, J., 2007, "***The Effect of Hot-Streaks on HP Vane Surface and Endwall Heat Transfer: An Experimental and Numerical Study***", Journal of Turbomachinery, **129**(1): pp. 32-43.
19. Povey, T. and Qureshi, I., 2009, "***Developments in Hot-Streak Simulators for Turbine Testing***", Journal of Turbomachinery, **131**(3) (031009).
20. Pau, M., Paniagua, G., Delhaye, D., and de La Loma, A., 2008, "***Aerothermal Impact of Stator-Rim Flow and Rotor Platform Film Cooling on a Transonic Turbine stage***". GT2008-51295, ASME Turbo Expo 2008, Berlin, Germany.
21. Mathison, R.M., Haldeman, C.W., and Dunn, M.G., 2010, "***Heat Transfer for the Blade of a Cooled Stage and One-Half High-Pressure Turbine, Part I: Influence of Vane Cooling and Disk Cavity Purge Flow***". GT2010-22713, ASME Turbo Expo, Glasgow, Scotland.
22. Mathison, R.M., Haldeman, C.W., and Dunn, M.G., 2010, "***Aerodynamics and Heat Transfer for a Cooled One and One-Half Stage High-Pressure Turbine--Part I: Vane Inlet Temperature Profile Generation and Migration***". GT2010-22716, ASME Turbo Expo 2010, Glasgow, Scotland.
23. Mathison, R.M., "***Experimental and Computational Investigation of Inlet Temperature Profile and Cooling Effects on a One and One-Half Stage high Pressure Turbine Operating at Design Corrected Conditions***", Ph.D. dissertation, Department of Mechanical Engineering, Ohio State University, 2009, pp. 370.
24. Haldeman, C.W., Mathison, R.M., and Dunn, M.G., 2004, "***Design, Construction and Operation of a Combustor Emulator for Short-Duration High-Pressure Turbine Experiments***". AIAA-2004-3829, AIAA Joint Propulsion Conference, Ft. Lauderdale, FL.
25. Hodak, M.P., "***Qualification of Fourth Generation Kapton Heat-flux Gauge Calibration Performance***", Masters, Department of Mechanical Engineering, Ohio State University, 2010, pp. 81.
26. Cohen, B., "***Numerical and Experimental Investigation of Unsteady Heat-Transfer Data Reduction Algorithms***", Department of Mechanical Engineering, Ohio State University, 2005, pp. 112.
27. Kahveci, H.S., "***The Influence of Film Cooling and Inlet Temperature Profile on Heat Transfer for the Vane Row of a 1-1/2 Stage Transonic High-Pressure Turbine***", Ph.D. Dissertation, Department of Mechanical Engineering, Ohio State University, 2010, pp. 286.
28. Mathison, R.M., Wishart, M.B., Haldeman, C.W., and Dunn, M.G., 2010, "***Temperature Predictions and Comparison with Measurements for the Blade Leading Edge and Platform of a 1-1/2 Stage Transonic HP Turbine***". GT2010-22987, ASME Turbo Expo 2010, Glasgow, Scotland.